Investigation on Radio Wave Propagation in Shallow Seawater: Simulations and Measurements

Eugenio Jimenez, Gara Quintana, Pablo Mena, Pablo Dorta and Ivan Perez-Alvarez
Institute for Technological Development and Innovation in Communications (IDeTIC),
Universidad de Las Palmas de Gran Canaria,
Las Palmas, 35017, Spain.
e-mail: eugenio.jimenez@ulpgc.es

Santiago Zazo, Marina Perez
ETSI Telecomunicacion,
Universidad Politecnica de Madrid,
Madrid 28040, Spain.
e-mail: santiago@gaps.ssr.upm.es
e-mail: marina.perez@isom.upm.es

Eduardo Quevedo
Oceanic Platform of the Canary Islands (PLOCAN),
Telde 35200, Spain.
e-mail: eduardo.quevedo@plocan.eu

***Abstract*—The authors present full wave simulations and experimental results of propagation of electromagnetic waves in shallow seawaters. Transmitter and receiver antennas are ten-turns loops placed on the seabed. Some propagation frameworks are presented and simulated. Finally, simulation results are compared with experimental ones.**

***Index Terms*—Conducting medium; underwater loop antennas; EM wave propagation; shallow seawaters.**

I. Introduction

ELECTROMAGNETIC propagation through sea water is very different from propagation through air because of water's high permittivity and electrical conductivity. Plane wave attenuation is higher through water, and increases rapidly with frequency. With a relative permittivity of about ϵ_r=80, water has the highest permittivity of any material and this has a significant impact on the angle of refraction at the air/water interface. Conductivity of seawater is typically around 5S/m, while nominally fresh water conductivity is quite variable but typically in the mS/m range. Relative permeability is approximately μ_r=1 so there is little direct effect on the magnetic field component but conduction leads to strong attenuation of electromagnetic propagating waves.

Another important consideration is the effect of the air-to-water interface. Propagation losses and the refraction angle are such that an electromagnetic signal can cross the air-to-water boundary and appears to radiate from an antenna directly placed in the air above the transmitter [1]. This effect aids communication from a submerged station to land and between shallow submerged stations without the need for surface repeater buoys. The air path can be a key advantage. For example, if two divers are 1km apart at 2m below the surface, attenuation will be significantly less than anticipated from the 1km through-water loss.

A similar effect is seen at the seabed, where its conductivity is lower than the water one. The seabed is an alternative low-loss, low-noise, communications path if both transmitter and receiver are placed on the seabed.

978-1-5090-2696-8/16/$31.00

In many deployments a single propagation path will be dominant depending on the placement of transmitter and receiver. In our case both transmitting and receiving antennas will be placed on the seabed as it is illustrated in Fig 1.

Full wave analysis of propagating EM waves in two-layers geometries was firstly carried out by A. Sommerfeld at the begining of the XX century. Later, his work was extended to multilayer geometries and in [2], [3], [4], [5] and [6] full wave analysis of geometries with two, three and more layers and applications are well summarized.

Channel characterization for underwater communications using EM modelling is studied in [7], [8], [9] and [10].

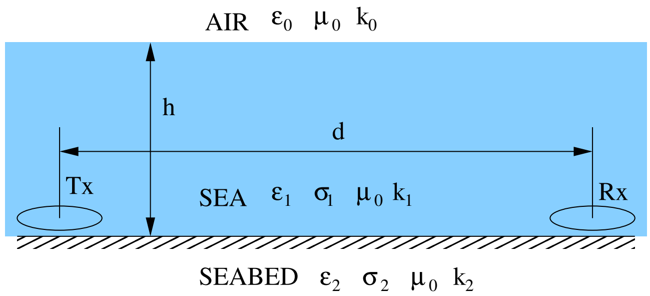

Fig. 1. Geometric configuration of testbed.

II. Simulation Frameworks

Along this communication, four different frameworks are going to be simulated.

- Attenuation between two horizontal loops placed in free space.
- Attenuation between two horizontal loops inmersed in sea water.
- Attenuation between two horizontal loops placed on seabed to sea water interface without air layer; two layers problem.
- Attenuation between two horizontal loops placed on seabed to sea water interface with an air layer over sea water; three layers problem.

In all cases, transmitter and receiver antennas are of the same kind: a 22cm. radius ten turns loop antenna made of copper and isolated using a 1mm. teflon like coating. Sea water is modelled as a dielectric with permittivity ϵ_r=81 and conductivity σ=4.5 S/m. Seabed, fine sand, is modelled as a dielectric with permittivity ϵ_r=3.5 and conductivity σ=1 S/m [11]. Height of sea water layer is set to h=4 m.

Simulations are carried out using a commercial MoM solver: FEKO [12]. This tool supports the features needed for this analysis: planar Green functions for multilayered media, dielectric coated wires and special basis functions for low frequency analysis.

Simulations are carried out at five different distances (d=2, 3, 4, 5 and 6 meters) with frequency sweeps from 10 kHz to 1 MHz.

III. Simulation Results

A. Antennas inmersed in homogeneous medium

In these simulations, antennas are radiating into two homogeneous mediums: free space and sea water. Results of those simulations are shown in Fig 2 and in Fig 3.

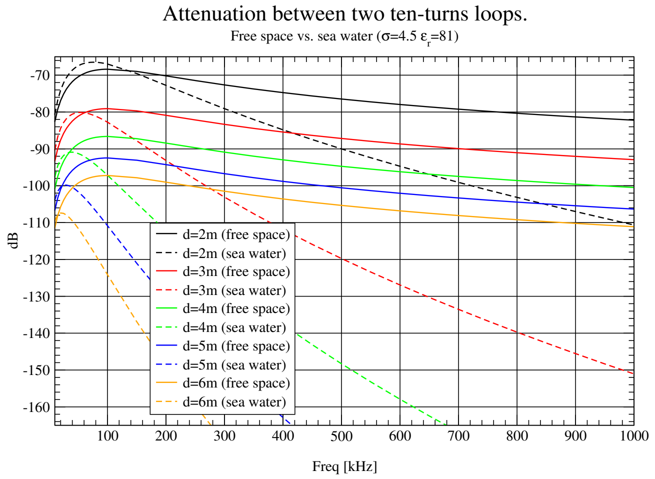

Fig. 2. Free space vs. sea water. Full sweep.

As it is expected for antennas inmersed in sea water, attenuation grows exponentially with frequency due to sea water conductivity (attenuation constant $\alpha = \sqrt{\frac{\sigma\omega\mu}{2}}$ Neper/m). This is true for frequencies over 100 kHz but not for frequencies between 10 kHz and 100 kHz. For low frequencies and distances or for very low frequencies, attenuation decreases with frequency in both cases: free space and sea water, and it seems to be independent of the electrical properties of the medium. In this case a magnetostatic approach can explain this behaviour.

For antennas in free space and frequencies over 100 kHz, attenuation for each frequency increases 18 dB when doubling distance. It is a typical near field dependence (eg $1/R^3$).

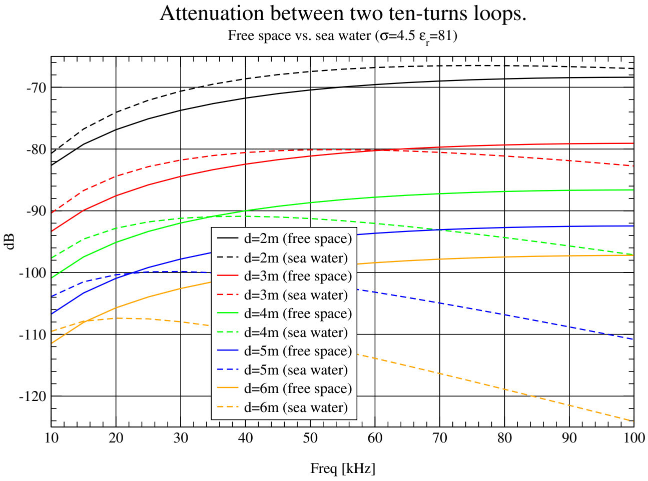

Fig. 3. Free space vs. sea water. Low frequency sweep.

Electrically small loop antennas work as vertical magnetic dipoles. The electromagnetic fields generated by this source [2] are (cylindrical coordinates):

$$B_\rho = \frac{1}{4\pi\omega}\frac{\rho z}{r^2}\left(\frac{jk^2}{r} - \frac{3k}{r^2} - \frac{3j}{r^3}\right)e^{jkr}$$

$$B_z = -\frac{1}{4\pi\omega}\left[\frac{jk^2}{r} - \frac{k}{r^2} - \frac{j}{r^3} - \frac{z^2}{r^2}\left(\frac{jk^2}{r} - \frac{3k}{r^2} - \frac{3j}{r^3}\right)\right]e^{jkr}$$

$$E_\phi = -\frac{1}{4\pi}\frac{\rho}{r}\left(\frac{jk}{r} - \frac{1}{r^2}\right)e^{jkr}$$

These equations clearly show the aforementioned behaviours: mainly magnetic field for low frequencies and distances and $1/R^3$ near field dependence for low distances.

B. Antennas inmersed in layered medium

Now we are going to compare the results from simulation of antennas in sea water with simulations of antennas placed on seabed. Both layers, sea water and seabed, are semi-infinite so it is a two layer geometry.

Results of those simulations are shown in Fig 4 and in Fig 5.

As it can be seen, the effect of seabed layer is to decrease the attenuation at all frequencies. This could mean that energy is mainly travelling on the sea-seabed interface. Once again, for low frequencies and distances or for very low frequencies, attenuation seems to be independent from the medium.

Full expressions for the fields generated by a vertical dipole placed on the interface between two mediums can be found in [2] and in [13]. We are not going to reproduce them here because of their length and complexity.

Simulations with three layers (seabed, sea water and air) has been carried out too. Results of those simulations, with water height h=4m, are indistinguishable from those of the two layers. So, at least for our testbed, the seawater to air interface seems not to have any effect.

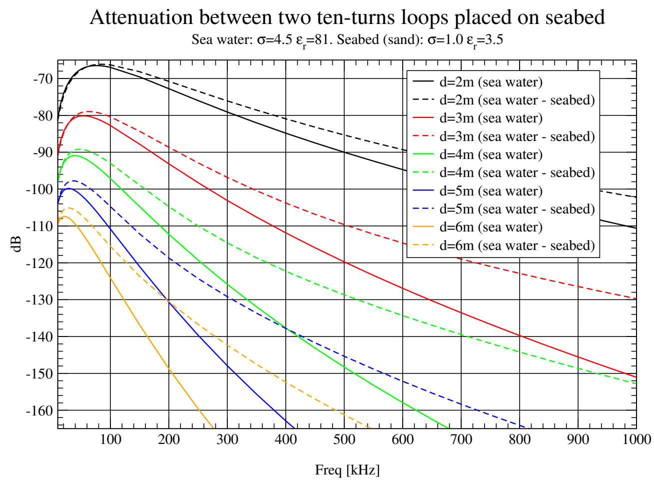

Fig. 4. Sea water vs. two layer. Full sweep.

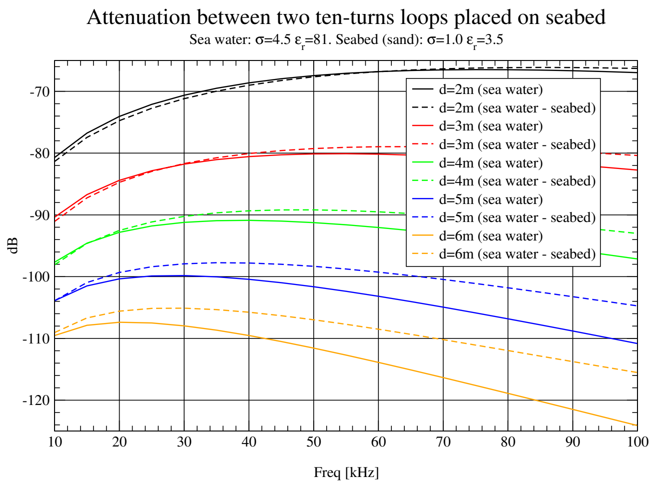

Fig. 5. Sea water vs. two layer. Low frequency sweep.

IV. Experimental Results

After reviewing a great number of studies about underwater propagation, we have found little information about experimental results in this frequency band. Therefore, a measurement system was designed and several experiments were carried out along 2015 and 2016. After debugging a lot of problems we came to a conclusion: the only way to measure without interferences in this band was to **submerge all of the equipment in the sea** and communicate with it using a fiber link. No copper cables from undersea to ground, even coaxial ones work like antennas.

The selected location is in Taliarte Harbour (Telde, Canary Islands, Spain). This location was selected because PLOCAN's headquarters are placed there and we can use a private pier. The testbed is shown in Fig 6 and a photograph of both systems is shown in Fig 7.

A full description and details of the design of the experimental seabed can be found in [14].

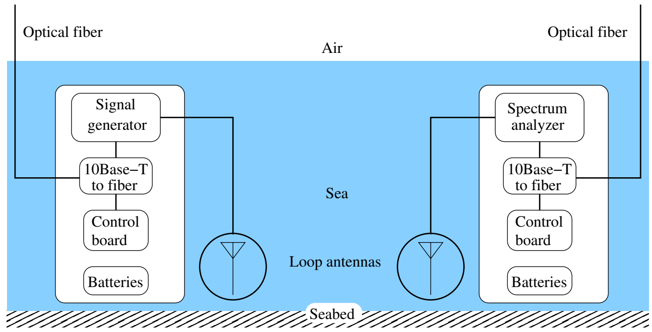

Fig. 6. Experimental testbed setup.

A. Transmitter and antenna

The transmitter is built using a Keysight 33220A waveform generator, a Beaglebone Black board, a 10Base-T to fiber transceiver and a battery pack with an inversor. All the equipment is placed into a receptacle made of high pressure PVC pipe. The loop antenna is made of enamelled coper covered with self-vulcanizing tape and it ts conected to the transmitter using a short patch of coaxial line. The PVC receptacle is pressurized and the control board sends information about pressure and temperature using the fiber link. The generator is controlled from an external computer using Keysight VEE software.

B. Receiver and antenna

The receiver is built using a handheld Keysight 9340B spectrum analyzer, a Beaglebone Black board, a 10Base-T to fiber transceiver and a battery pack. All the equipment is placed into a receptacle made of high pressure PVC pipe. The loop antenna is the same used in the transmitter and the PVC receptacle is pressurized too. The analyzer is controlled from an external computer using Keysight VEE software.

Fig. 7. Transmitter and receiver.

C. Results

Frequency sweeps were made between 10 kHz and 100 kHz (1 kHz IF bandwidth) and between 100 kHz and 1 MHz (3 kHz IF bandwidth). Both antennas were placed on the seabed and the distance between their centers was swept between 2 and 6 meters using one meter steps. Signal generator power was set to 18 dBm for distances between 2 and 5 meters. For 6 meters, signal generator power was set to 23 dBm.

After making the measurements, data from the spectrum analyzer needs to be calibrated with a well known source. The spectrum analyzer has a poor response below 40 kHz (it's rated for use from 100 kHz) and calibration curves have to be made in the lab to improve its response. These curves help extracting the effects of analyzer in the measurements.

In Fig 8 a full sweep between 10 kHz and 1 MHz is shown. In this figure, simulations of a two layer model (water-seabed) are compared with measurements. Heigth of water was four meters during the measurements.

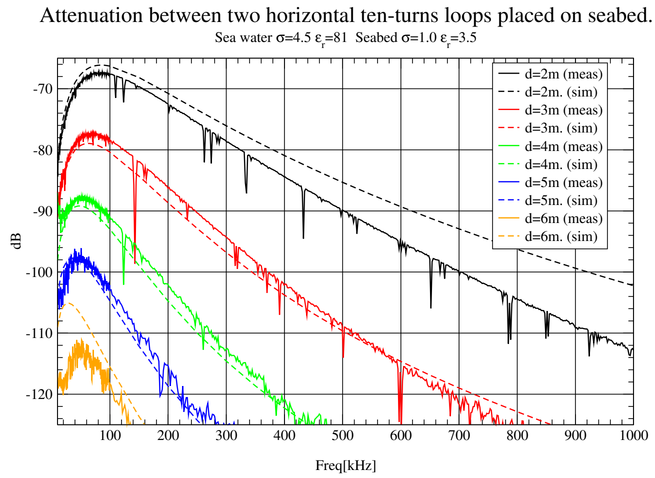

Fig. 8. Measurements vs. simulations. Full sweep.

In Fig 9 a low frequency sweep between 10 kHz and 100 kHz is shown. Results for 4, 5 and 6 meters and for frequencies below 40 kHz are largely influenced by the response of the spectrum analyzer at low power levels at these frequencies. A new spectrum HF analyzer from Aaronia GmbH (1 Hz to 30 Mhz) has been acquired and a new measurement campaign is being planned as of writing this paper.

V. Conclusions

This paper investigates the propagation of EM waves generated by loop antennas horizontally placed on seabed at different frequencies and distances. Full wave simulations and measurements are carried out for the same testbed geometry and two conclusions can be drawn.

First, simulations predict that for frequencies over 100 kHz propagation takes place mainly on the seabed-seawater interface. The simulated attenuation is greater in an homogeneous medium (seawater) than in a two layer medium (seawater-seabed). These predictions agreed with the measurements.

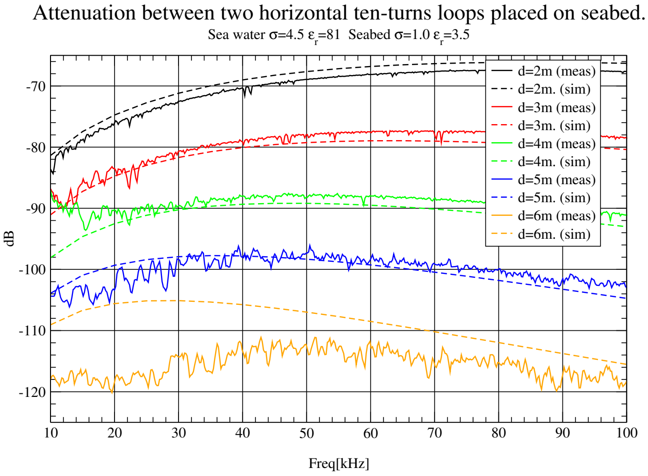

Fig. 9. Measurements vs. simulations. Low frequency sweep.

Second, simulations predict that for low frequencies the influence of the medium decreases with the frequency showing a behaviour that can be explained using a magnetostatic approach. This effect is stronger at short distances. These predictions agree with the measurements too.

Atenuattion measurements sweeping frequencies and distances are very scarce in the available literature for this field and we think this is the main contribution of this work. We could not find similar measurements in the literature we reviewed.

The good agreement between simulations and measurements validates the simulation tool. It will let us to make "numerical" experiments with antenna placement (vertical, horizontal, etc...), with antenna geometry (radius of the loop, number of turns, shape, etc...) and with frequency choice.

Acknowledgment

The authors would like to thank the work carried out by Juan Domingo Santana Urbin (ULPGC) when making the pressurized PVC receptacles, loop antennas and all of the lab stuff needed to make the measurements. Also, the authors would like to thank the work carried out by Gabriel Juanes and Raul Santana (PLOCAN) when setting up measurement testbed in the pier and into the sea.

This work has been supported by Ministerio de Economia y Competitividad, Spain, under public contract TEC2013-46011-C3-R.

References

[1] J. Lucas and C. Yip, "A determination of the propagation of electromagnetic waves through seawater," *Underwater Technology*, vol. 27, no. 1, pp. 1–9, Feb 2007.

[2] R. W. King, M. Owens, and T. T. Wu, *Lateral Electromagnetic Waves*. New York, NY, USA: Springer-Verlag, 1992.

[3] J. R. Wait, *Electromagnetic Waves in Stratified Media*, ser. IEEE/OUP series on electromagnetic wave theory, J. B. Anderson, Ed. Piscataway, NJ, USA: IEEE Press and Oxford Univeristy Press, 1996.

[4] K. Li, *Electromagnetic Fields in Stratified Media*. Hangzou, China, Berlin, Germany: Zhejiang University Press and Springer-Verlag GmbH, 2009.

[5] H. Wang, K. Zheng, K. Yang, and Y. Ma, "Electromagnetic field in air produced by a horizontal magnetic dipole immersed in sea: Theoretical analysis and experimental results," *IEEE Transactions on Antennas and Propagation*, vol. 62, no. 9, pp. 4647–4655, Sept 2014.

[6] W. Honglei, Y. Kunde, and Z. Kun, "Performance of dipole antenna in underwater wireless sensor communication," *IEEE Sensors Journal*, vol. 15, no. 11, pp. 6354–6359, Nov 2015.

[7] C. W. Kim, E. Lee, and N. A. A. Syed, "Channel characterization for underwater electric conduction communications systems," in *OCEANS 2010 MTS/IEEE SEATTLE*, Sept 2010, pp. 1–6.

[8] V. P. Bui and W. S. Yeoh, "Propagation and channel characteristics in seawater environment," in *2014 IEEE Antennas and Propagation Society International Symposium (APSURSI)*, July 2014, pp. 701–702.

[9] N. Pelavas, G. J. Heard, and G. Schattschneider, "Development of an underwater electric field modem," in *2014 Oceans - St. John's*, Sept 2014, pp. 1–5.

[10] A. Zoksimovski, D. Sexton, M. Stojanovic, and C. Rappaport, "Underwater electromagnetic communications using conduction channel characterization," *Ad Hoc Networks*, vol. 34, pp. 42 – 51, 2015, advances in Underwater Communications and Networks. [Online]. Available: http://www.sciencedirect.com/science/article/pii/S157087051500027X

[11] U. M. Cella, R. Johnstone, and N. Shuley, "Electromagnetic wave wireless communication in shallow water coastal environment: Theoretical analysis and experimental results," in *Proceedings of the Fourth ACM International Workshop on UnderWater Networks*, ser. WUWNet '09. New York, NY, USA: ACM, 2009, pp. 9:1–9:8. [Online]. Available: http://doi.acm.org/10.1145/1654130.1654139

[12] Altair. Feko computational electromagnetics code. [Online]. Available: http://www.altairhyperworks.com/product/FEKO

[13] D. Margetis and T. T. Wu, "Exactly calculable field components of electric dipoles in planar boundary," *Mathematical Physics*, vol. 42, pp. 713–745, feb 2001.

[14] P. Mena, P. Dorta, G. Quintana, E. Jimenez, I. Perez, S. Zazo, M. Perez, L. Cardona, and J. Brito, "Experimental testbed for seawater channel characterization," submitted to UComms '16 Proceedings of the Third Underwater Communications Conference, 2016.